Acta Oceanol. Sin., 2024, Vol. 43, No. 4, P. 105–118
https://doi.org/10.1007/s13131-024-2338-3
http://www.aosocean.com
E-mail: ocean2@hyxb.org.cn

Structural characteristics and tectonic division of the Zambezi Delta basin in the offshore East Africa: evidences from gravity and seismic data

Guozhang Fan[1†], Wen Li[2†], Liangbo Ding[1], Wanyin Wang[2, 3, 4*], Hongping Wang[1], Dingding Wang[2, 5], Lin Li[1], Hao Wang[2], Chaofeng Wang[1], Qingluan Wang[2], Ying Zhang[1]

[1] Hangzhou Research Institute of Petroleum Geology, PetroChina, Hangzhou 310023, China

[2] College of Geological Engineering and Geomatics, Chang'an university, Xi'an 710054, China

[3] Key Laboratory of Marine Geology and Environment, Chinese Academy of Sciences, Qingdao 266071, China

[4] National Engineering Research Center of Offshore Oil and Gas Exploration, Beijing 100028, China

[5] Department of Earth, Environment and Resources Sciences, University of Naples Federico Ⅱ, Naples 80138, Italy

Received 1 August 2023; accepted 15 April 2024

Abstract

The Zambezi Delta basin is a passive marginal basin located on the East African coast that has good oil and gas exploration potential. Due to the special geological evolutionary background of the Beira High in the Zambezi Delta basin, it has a low gravity anomaly, and the existing seismic survey lines do not cover the whole basin; therefore, it is difficult to interpret the structural characteristics of the whole basin based solely on gravity or seismic data. Based on satellite altimetry gravity anomaly data, this study infers the distribution characteristics of faults in the Zambezi Delta basin by using the normalized vertical derivative of the total horizontal derivative (NVDR-THDR) technique. Then, constrained by seismic data, the gravity anomaly at the Moho interface is extracted by using the fast forward method of the double-interface model of the gravity anomaly, and this anomaly is then removed from the Bouguer gravity anomaly to obtain the sedimentary layer gravity anomaly. The thickness of the sedimentary strata is obtained by inversing the sedimentary basement depth of the whole basin. Then, uplifts and depressions are divided based on a sedimentary layer thickness of 3 km. This research demonstrates that the Zambezi Delta basin mainly features nearly SN-trending and NE-trending faults and that these faults exhibit east-west partitioning. The nearly SN-trending strike-slip faults controlled the sedimentary development of the basin, and the NE-trending tensile faults may have acted as migration channels for oil, gas and magma. The "overcompensation" effect of the Moho interface gravity anomaly on the gravity anomaly of the sedimentary layer is caused by the depression of the Moho interface beneath the Beira High, which results in a low gravity anomaly value for the Beira High. The pattern of uplifts and depressions trends NE and has the structural characteristics of east-west blocks.

Key words: Zambezi Delta basin, satellite altimetry gravity anomaly, Beira High, fault division, uplift and depression pattern

Citation: Fan Guozhang, Li Wen, Ding Liangbo, Wang Wanyin, Wang Hongping, Wang Dingding, Li Lin, Wang Hao, Wang Chaofeng, Wang Qingluan, Zhang Ying. 2024. Structural characteristics and tectonic division of the Zambezi Delta basin in the offshore East Africa: evidences from gravity and seismic data. Acta Oceanologica Sinica, 43(4): 105–118, doi: 10.1007/s13131-024-2338-3

1 Introduction

China is a major producer and consumer of oil and gas.Since becoming a net importer of oil and gas in 1993, its dependence on foreign countries has continuously increased. With the rapid growth of China's demand for oil and gas resources, overseas oil and gas resources have become indispensable sources of oil and gas in China, and strengthening overseas oil and gas exploration is crucial for ensuring China's national energy security (Zhang et al., 2022).

The Zambezi Delta basin in the passive marginal basin of East Africa is located on the western shore of the Indian Ocean and lies southeast of Africa. It is adjacent to the Mozambique Fold Belt to the north, the Morondava Basin across the Mozambique Channel to the east, the Mozambique Sea Basin to the south, and the Mozambique Basin to the west (Fig. 1). In the northern part of the basin, a magmatic intrusion formed the Limpopo-Angoche dike (Cox, 1992; Jourdan et al., 2007, 2009; Li, 2021), and the eastern and western sides are controlled by the David Fault Zone (DFZ) and the Mozambique Fault Zone (MFZ) respectively, therefore this basin has featured a relatively stable sedimentary environment. The widely developed pro-delta and marine shales in the basin have good hydrocarbon generation potential as source rocks. The Cretaceous–Paleocene sandstones directly overlying the source rocks act as reservoirs, and the marine Crudji Formation shale acts as a good cap layer. Additionally, faults have provided good migration channels into composite traps

Foundation item: The Petrochina Basic Prospective Science and Technology Research Project–Overseas deepwater ultra-deepwater oil and gas exploration technology research topic, under contract No. 2021DJ2403.

*Corresponding author, E-mail: wwy7902@chd.edu.cn

†These authors have contributed equally to this word.

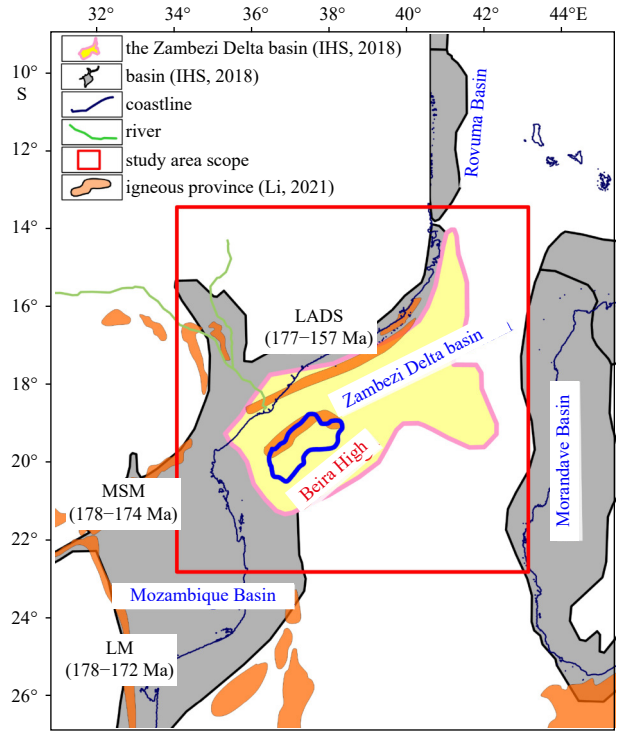

Fig. 1. Regional geology.

formed by a combination of strata and structures. The relatively stable sedimentary environment and good combination of source, reservoir and cap in the Zambezi Delta basin result in enormous potential for oil and gas exploration (Jin et al., 2012; Mahanjane, 2014; Solomon et al., 2014; Wen et al., 2015; Cui et al., 2016, 2020; Shi et al., 2023), and this basin has been further classified as a strategic preparation area for oil and gas strategic exploration in deep-water basins on the East African continental margin (Zhang et al., 2022). The structural characteristics of the basin reflect its sedimentary evolution to a certain extent. The formation of muddy shales, sandstones and shales by sedimentary processes was closely related to the generation and accumulation of oil and gas. Therefore, studying the characteristics of faults and the pattern of uplifts and depressions in the Zambezi Delta basin can improve the understanding of the distribution patterns of oil and gas and is highly important for guiding oil and gas exploration.

Recently, a series of studies have been carried out in the Zambezi Delta basin; however, the distribution characteristics of faults and uplift and depression patterns are relatively few. In research on the faults in the Zambezi Delta basin, previous studies have focused mainly on analyzing the vertical distribution characteristics of faults using two-dimensional seismic profile data (Salman and Abdula, 1995; Mahanjane, 2012; Mahanjane et al., 2014; Castelino et al., 2015). Furthermore, several scholars have used seismic and geological profile data not only to analyze the vertical distribution characteristics of faults, but also to study the geological characteristics, structural evolution, oil and gas prediction and other fields of the Zambezi Delta basin (Xu et al., 2014; Mahanjane et al., 2014; Solomon et al., 2014; Yu et al., 2015; IHS, 2018; Ponte et al., 2019; Cui et al., 2020). Compared to this, relatively little research has been conducted on the lateral distribution characteristics of faults. IHS (2018) identified NE-trending faults in the western Zambezi Delta basin. Based on the interpretation of seismic data, Mahanjane (2012) analyzed nearly NE-trending faults formed by weak tectonic deformation on the northern and southern sides of the Beira High. Based on the reconstruction of the southward drift of Antarctica relative to Africa, Senkans et al. (2019) analyzed the formation and evolution of the Zambezi Delta basin and described the distribution characteristics of the faults: nearly NE-trending tensile faults developed mainly in the area to the north of the Beira High, and NW-trending transitional faults developed on the western and eastern sides of the Beira High. In research on the tectonic division of the Zambezi Delta basin, most studies have used two-dimensional seismic data to identify the uplift and depression patterns in the profile locations (Watts, 2001; Leinweber et al., 2013; Xu et al., 2014; Castelino et al., 2015; Mueller et al., 2016; Mueller and Jokat, 2017, 2019; Ponte et al., 2019; Cui et al., 2020). However, few studies have focused on the tectonic characteristics of the entire basin. IHS (2018) divides the Zambezi Delta basin into a tectonic pattern composed of two depressions surrounding one uplift, i.e., the northern delta, the central Beira High and the southern submarine fan. König and Jokat (2010) used magnetic anomaly characteristics to identify the oceanic and continental boundaries between the Zambezi Delta basin and the Mozambique Sea basin. On this basis, the margins of the Beira High, Nemo High and nearshore depression in the basin were described (Mahanjane, 2012); unfortunately, this study focused mainly on the tectonic evolution, and these regions are only generally described. Multiple two-dimensional seismic profiles and gravity anomaly data were used to infer the sedimentary thickness near the profile area, and the uplift and depression in the region were also described (Castelino et al., 2015). On the basis of the results of previous studies, Senkans et al. (2019) reconstructed the southward drift of the Antarctic plate relative to the African Plate, further clarified the tectonic evolution model and identified the approximate location of the oceanic–continental transition (OCT) and seaward-dipping reflectors (SDRs) in the basin.

This summarization of previous studies on the structural characteristics and tectonic division of the Zambezi Delta basin suggests that the following problems still exist: (1) fault studies have focused mainly on analyzing the vertical distribution characteristics in seismic profiles; compared to these studies, relatively little research has been conducted on the lateral distribution characteristics. (2) The study of the tectonic division has focused mainly on the vertical distribution characteristics through the use of seismic and geological profiles. Laterally, the special geological evolutionary background of the Beira High results in a low gravity anomaly, which makes it difficult to study tectonic characteristics with gravity data, and the available seismic data do not cover the entire basin; thus, research on the tectonic pattern of the whole basin is relatively limited. Gravity data have the advantages of easy acquisition, high lateral resolution and wide coverage area. Therefore, on the basis of previous studies on faults and tectonic patterns in the Zambezi Delta basin, this paper identifies faults in the study area based on gravity anomaly data. In view of the special geological phenomenon of a low gravity anomaly in the Beira High, this paper proposes a set of schemes for inversing the thickness of the sedimentary layer under the constraints of seismic data and subsequently describing the tectonic pattern. On this basis, combined with a hydrocarbon accumulation model and the distribution of oil and gas wells in the Zambezi Delta basin, a comprehensive analysis of the structural pattern and oil and gas distribution is conducted.

2 Data sources and research methods

2.1 *Physical properties of the rocks*

Obtaining accurate physical properties is the premise of geophysical data processing and interpretation. This paper reviews and summarizes the existing research results on the physical properties of the rocks in the study area (Table 1, Leinweber et al., 2013). The average density values of 2.43×10^3 kg/m^3, 2.55×10^3 kg/m^3, and 2.98×10^3 kg/m^3 were taken as the mean densities of sediment layer 3, sediment layer 5, and the lower crust, respectively. Based on the collected sedimentary layer thickness and density information, sedimentary layers 1 to 4 are classified as Cenozoic strata, while sedimentary layers 5 to 8 are classified as Mesozoic strata. It is inferred that several prominent density layers are distributed from top to bottom in the study area, and the weighted average density calculation formula $\bar{\sigma} = \frac{\sum_i d_i \times \sigma_i}{\sum_i d_i}$, is used to calculate the density of each layer with the following values: a water layer density of 1.03×10^3 kg/m^3, a Cenozoic strata density of 2.30×10^3 kg/m^3, a Mesozoic strata density of 2.60×10^3 kg/m^3, a crust density of 2.90×10^3 kg/m^3, and a mantle density of 3.27×10^3 kg/m^3.

2.2 *Topographic and gravity data*

The topographic elevation (Fig. 2) and satellite altimetry gravity anomaly data (Fig. 3) used in this study area were obtained from the Global Satellite Altimetry Gravity Database (https://topex.ucsd.edu/cgi-bin/get_data.cgi) and maintained jointly by David T. Sandwell (Scripps Institution of Oceanography, University of California) and Walter H. F. Smith (the National Oceanic and Atmospheric Administration Satellite Altimetry Laboratory). The global terrain database version is V23.1, and the data network size is 1′ × 1′. The Global Satellite Altimetry Gravity Database version is V31.1. In the sea area, the data network size is 1′ × 1′, and the accuracy is approximately ± 2 mGal, which can meet the gravity work requirements of 1:500 000 scale accuracy. In the land area, the data are a combination of satellite altimetry gravity

Table 1. Statistical table of the main strata densities (refer to Leinweber et al., 2013)

Main layer	Layer	Max thickness/km	Main density(10^3 kg · m^{-3})	Average density(10^3 kg · m^{-3})
Water layer	water layer	2.6	1.03	1.03
Cenozoic sediment layer	sediment layer 1	0.9	1.95	2.30
	sediment layer 2	0.8	2.18	
	sediment layer 3	1.8	2.39–2.46	
	sediment layer 4	1.8	2.40	
Mesozoic sediment layer	sediment layer 5	2.4	2.51–2.58	2.60
	sediment layer 6	1.3	2.62	
	sediment layer 7	0.9	2.60	
	sediment layer 8	2.6	2.64	
Crust	upper crust onshore	4.7	2.69	2.90
	middle crust onshore	32.0	2.91	
	lower crust	8.0	2.90–3.05	
Mantle	upper mantle	-	3.27	3.27

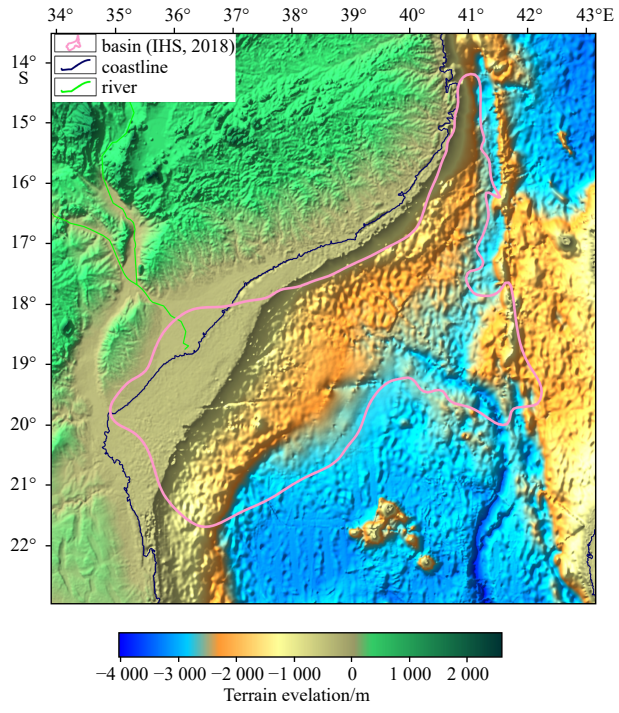

Fig. 2. Topographic map of the study area.

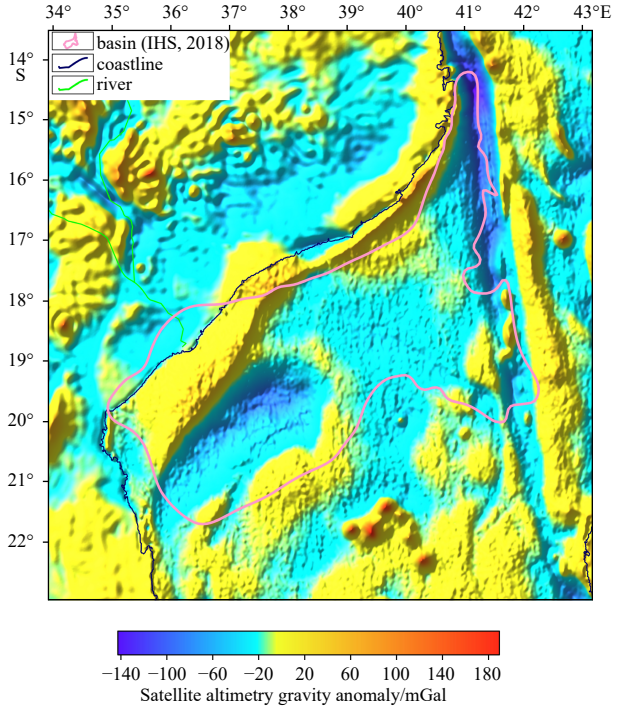

Fig. 3. Satellite altimetry gravity anomaly in the study area.

data, aerial gravity data and ground gravity data. The data network size is 5′ × 5′, and the accuracy is approximately ± 4 mGal, which can meet the gravity work requirements of 1:2 000 000 scale accuracy (Sandwell et al., 2014; He et al., 2023; Luo et al., 2023; Zhang et al., 2023). Sedimentary layer data were obtained from the global crustal model CRUST1.0 (https://igppweb.ucsd.edu/~gabi/crust1.html).

The majority of the Zambezi Delta basin lies below sea level, and the main interfaces are the bathymetric interface, Cretaceous top interface, Jurassic bottom interface and Moho interface from top to bottom. The satellite altimetry gravity anomaly (Fig. 3) represents the comprehensive response of the gravity anomalies caused by the uneven distribution of stratigraphic density and the fluctuations of these density interfaces. The terrain elevation difference in the study area reaches 6 500 m, and the satellite altimetry gravity anomaly is significantly influenced by the terrain, which is not conducive to the study of deep structures. Therefore, eliminating the influence of topography and bathymetry from the satellite altimetry gravity anomaly data is necessary.

To eliminate the influence of topography and bathymetry and obtain the Bouguer gravity anomaly, we adopted a generalized terrain correction technology based on the spherical coordinate system fan cylinder (Lei, 1984; An et al., 2010). An average crustal density of 2.90 × 10^3 kg/m^3 and a water layer density of 1.03 × 10^3 kg/m^3 were selected to calculate the Bouguer gravity anomaly in the study area (Fig. 4). The accuracy of the satellite altimetry gravity anomaly data in sea areas is greater than that in land areas; therefore, the accuracy of Bouguer gravity anomaly data in sea areas is still greater than that in land areas. The Bouguer gravity anomaly values in the study area range from −143 mGal to 305 mGal, and the overall trend is NE. Macroscopically, the Bouguer gravity anomaly is low in the northwest and high in the southeast. Along the eastern edge of the Zambezi Delta basin, a nearly SN-trending anomaly zone nearly crosses the study area, which destroys the continuity of the Bouguer gravity anomaly in the Zambezi Delta basin and the eastern side of the basin. The overall gravity anomaly in the basin exhibits continuous high values, but there are patches of low value areas in the western part of the basin.

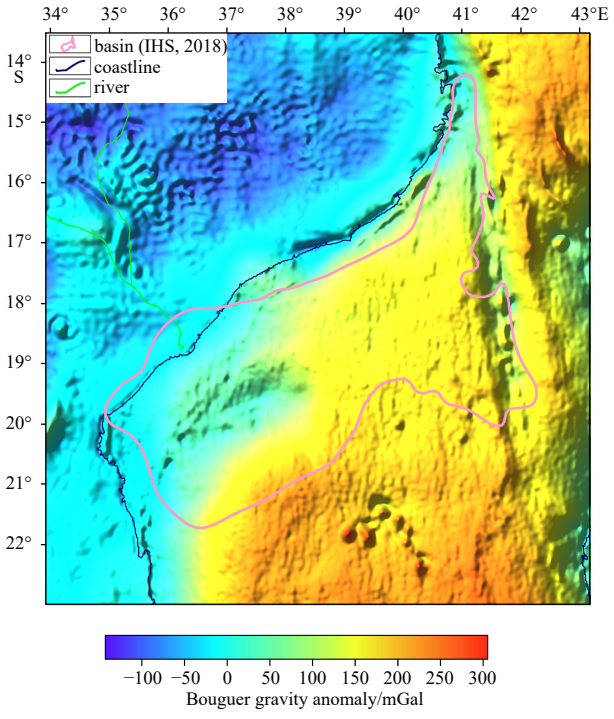

Fig. 4. Bouguer gravity anomaly in the study area.

2.3 *Seismic data*

The accuracy of inversion results may be affected by factors such as anomaly information extraction, the selection of density and the choice of inversion method during density interface inversion. To ensure that the inversion results more closely resemble real geological features, two interfaces formed by grid of constrained points is used for constrained inversion to improve the reliability of the inversion results. These constrained points were extracted from the 2D seismic profile data provided by the PetroChina Hangzhou Research Institute of Petroleum Geology. The distance between adjacent seismic profiles is approximately 50 km, and the minimum distance is up to 20 km. The profile accuracy is nearly 75 m, and some areas can reach up to 20 m. A total of 729 219 depth constraint points for the Cenozoic bottom interface and the Mesozoic bottom interface (both located within the profile range) were extracted respectively (the constraint points are shown in Fig. 5). After meshing, the Cenozoic bottom interface (Fig. 6) and Mesozoic bottom interface (Fig. 7) within the profile range are obtained and used for constrained inversion.

2.4 *Gravity data processing and interpretation techniques*

2.4.1 *Fault recognition method*

The deep and large faults in the Zambezi Delta basin are mostly tensile faults that formed during the Karoo intracontinental rift stage and the east-west Gondwana continental rift stage and were mainly generated by tensile stress. Due to the differences in shear resistance and tectonic stress, several strike-slip faults formed. Tensile and strike-slip faults can control the formation of different structural units on the two sides of the fault, destroy the continuity of the original strata, cause lateral differences in density on the two sides of the fault, and cause gradient zones or abnormal dislocations in the gravity anomaly data.

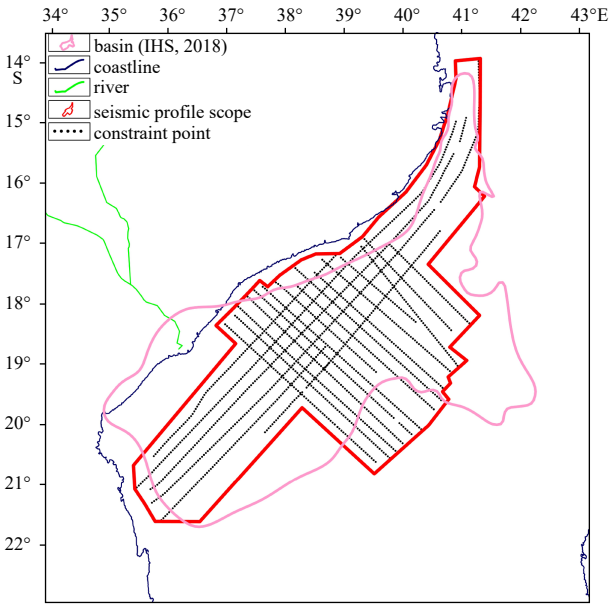

Fig. 5. Distribution of constraint points in the study area.

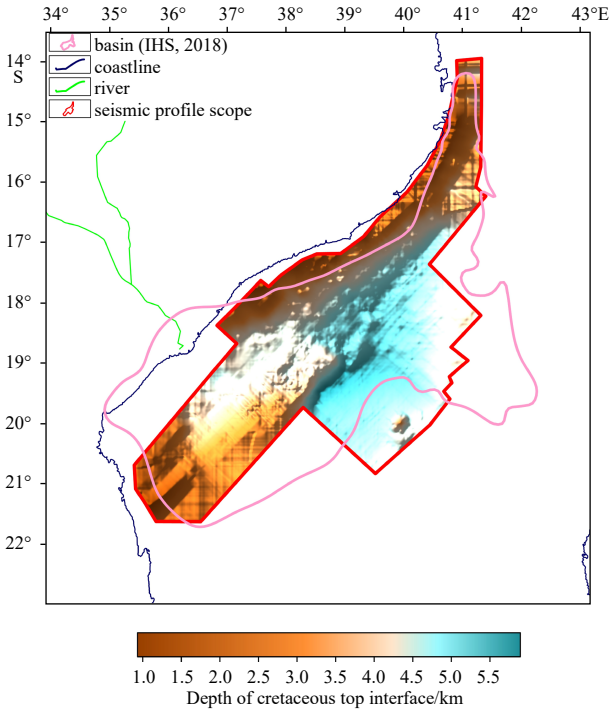

Fig. 6. Depth of the Cretaceous top interface in the study area.

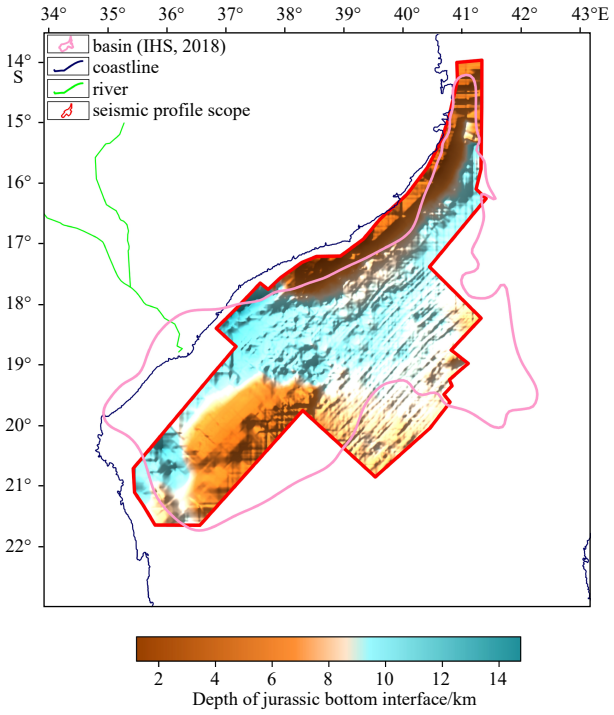

Fig. 7. Depth of the Jurassic bottom interface in the study area.

Therefore, the normalized vertical derivative of the total horizontal derivative (NVDR-THDR; Wang et al., 2009b) edge detection method can be used to identify the plane location of fault. In this study, we used the NVDR-THDR of the Bouguer gravity anomaly to identify the plane locations of fault. The main identifying characteristic of the tensile fault's plane location is a continuous ridge value of the NVDR-THDR. The faults are large in scale and nearly parallel to each other, but there are certain changes in the degree and trend of fault development. The main identifying characteristic of strike-slip fault is the plane dislocation of ridge value and the local continuous ridge value of the NVDR-THDR data. These faults are large in scale and have a great influence on the development of tension faults.

The Bouguer gravity anomaly NVDR-THDR data were obtained by calculating the normalized vertical derivative of the total horizontal derivative of the Bouguer gravity anomaly in the study area (Fig. 8). To verify the reliability of fault identification based on a ridge value in the NVDR-THDR data, a NE-trending seismic profile (the 2D seismic profile provided by the PetroChina Hangzhou Research Institute of Petroleum Geology, the location of which is shown by the purple solid line in Fig. 8) located in the Zambezi Delta basin was compared with the NVDR-THDR profile at the same location (Fig. 9). The ridge value in the NVDR-THDR data corresponds well with the location of the deep large faults that pass through the sedimentary layer on the western side of the Beira High, and it corresponds well with the boundary position of the Beira High and the basement fault with a high degree of throw on the Beira High. In the region west of the Beira

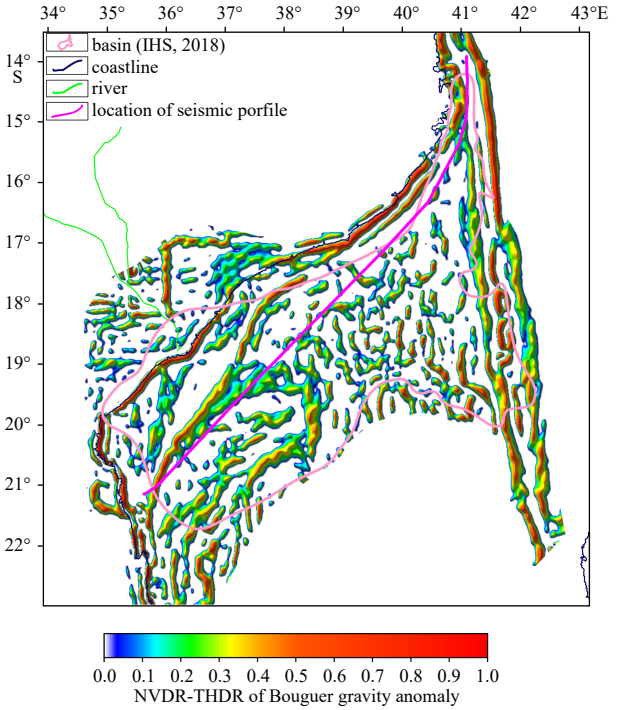

Fig. 8. NVDR-THDR of the Bouguer gravity anomaly and the location of the seismic profile in the study area.

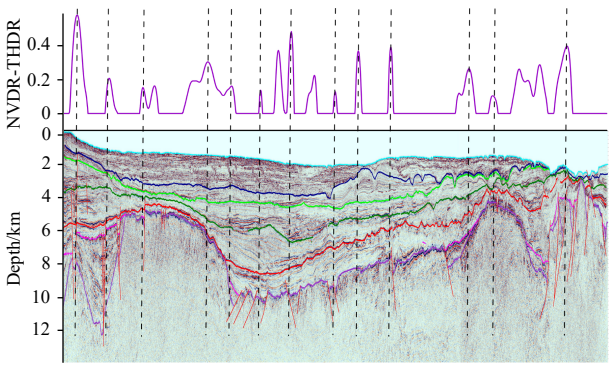

Fig. 9. Comparison of the NVDR-THDR of Bouguer gravity anomaly and the seismic profile.

High and east of the DFZ, the ridge value in the NVDR-THDR data corresponds well with the position of the basement fault at greater depths. However, basement faults at shallower depths produce smaller ridge values or have no ridge value of NVDR-THDR data. A possible reason is that the thicker sedimentary layers in this area have a certain shielding effect on the anomalies caused by basement faults, and the gravity anomaly response caused by the fault with a smaller scale is masked by the response from sedimentary layers, resulting in only a small reaction in the comprehensive response of the Bouguer gravity anomaly. In conclusion, the ridge value of NVDR-THDR data has a good correlation with the fault location in the seismic profile overall. Therefore, this study mainly uses the ridge value and its dislocations of the Bouguer gravity anomaly's NVDR-THDR data to identify the plane distribution characteristics of fault. In areas with poor continuity of ridge values in the NVDR-THDR data, the residual Bouguer gravity anomalies extracted by the method of minimum curvature potential field separation (Ji et al., 2015) are used for auxiliary identification, and the identifying characteristics are the zero value lines and their dislocations of residual gravity anomalies.

2.4.2 *Extraction method for gravity anomalies of sedimentary layers based on seismic constraints*

The Bouguer gravity anomaly is the comprehensive response of gravity anomalies generated by all uneven density geologic bodies inside the Earth. To obtain the gravity anomaly of sedimentary layers, it is necessary to extract the gravity anomaly of Moho interface first and then remove it from the Bouguer gravity anomaly. Therefore, accurately extracting the Moho gravity anomaly is the key to extracting the gravity anomaly of the sedimentary layers. One way to extract Moho interface gravity anomaly is direct filtering, which filters out Bouguer gravity anomalies directly according to the feature that the main frequency of gravity anomalies generated by geological anomalies at different burial depths differ (Ji et al., 2015; Xu et al., 2018; Rajesh et al., 2020); subsequently, the Moho interface gravity anomalies are extracted. However, all geological bodies can generate gravity anomaly signals across the full frequency band, and direct filtering of the Bouguer gravity anomaly signal not only eliminates local high-frequency signals caused by the Moho gravity anomaly but also introduces local low-frequency signals caused by other abnormal bodies. Therefore, extraction of Moho gravity anomalies by direct filtering is difficult. Another way is to forward model and peel off gravity anomalies layer by layer, that is, to forward model gravity anomalies caused by geological bodies in each layer based on prior information and then strip them layer by layer from the Bouguer gravity anomaly (Li et al., 2023). In this study, constraining points are extracted from seismic profile data, and the gravity anomalies caused by Cenozoic and Mesozoic strata are subjected to forward modeling via the fast forward method of the double-interface model of the gravity anomaly field (Wang and Pan, 1993) and are subsequently stripped layer by layer from Bouguer gravity anomalies; subsequently, the Moho gravity anomalies are extracted. The specific steps are as follows:

(1) Density interface data fusion. Because the seismic profile data do not cover the entire basin, the Cenozoic bottom interface (Fig. 6) and Mesozoic bottom interface (Fig. 7) are considered the basis for selecting suitable interfaces from the Crust1.0 model for interface fusion. Comparing the depths of various interfaces in the global crust model Crust1.0 with those of the Cenozoic and Mesozoic bottom interfaces obtained from seismic data, the mean square errors of the depth of the Cenozoic bottom interface relative to that of the Bottomsed1 interface and the depth of the Mesozoic bottom interface relative to that of the Bottomsed2 interface are minimal. Therefore, the Cenozoic and Mesozoic bottom interfaces extracted from the seismic data are fused with the Bottomsed1 and Bottomsed2 interfaces in the Crust1.0 model, after which the fused Cenozoic and Mesozoic bottom interfaces are obtained for the entire study area. Because the average depth difference between the Bottomsed2 interface and the bottom interface of the Mesozoic strata reaches 2.99 km, it is necessary to correct the Bottomsed2 interface with 2.99 km as the background value before fusion.

(2) Stripping the sedimentary layer gravity anomaly. This study is based on the fluctuating characteristics of the Cenozoic and Mesozoic fusion interfaces, the gravity anomalies of the Cenozoic and Mesozoic strata are forward modeled, and the anomalies are removed layer by layer from the Bouguer gravity anomaly. First, to forward the Cenozoic gravity anomaly, the zero plane is taken as the upper interface, and the fused Cenozoic bottom interface is taken as the lower interface. Taking -0.30×10^3 kg/m^3 as the residual density of Cenozoic strata relative to Mesozoic strata, the Cenozoic gravity anomaly relative to the Mesozoic gravity anomaly is calculated by using the fast forward method of the double-interface model of the gravity anomaly (Wang and Pan, 1993). Then, after forward modeling of the Mesozoic gravity anomaly, the zero plane is the upper interface, the fused Mesozoic bottom interface is the lower interface, and -0.30×10^3 kg/m^3 is the residual density of the Mesozoic strata relative to the crust. We calculate the gravity anomaly in the Mesozoic strata relative to the crust by using the fast forward method of the double-interface model of the gravity anomaly field (Wang and Pan, 1993). The Cenozoic and Mesozoic gravity anomalies are subtracted from the Bouguer gravity anomaly to highlight the gravity anomaly response of the Moho interface and other incompletely unstripped sedimentary strata.

(3) Extracting the Moho interface gravity anomaly. When stripping the sedimentary layer gravity anomaly, influenced by the accuracy of the fused geological interface and the selection of the normal density as the residual density of the strata, there are still gravity anomalies caused by local geological interface fluctuations and abnormal densities in the sedimentary layer. These gravity anomalies are collectively referred to the sedimentary layer gravity anomalies that are not completely stripped away. To accurately extract the Moho gravity anomaly, appropriate potential field separation parameters must be selected to remove gravity anomalies from sedimentary strata that are not completely stripped away, after which the Moho gravity anomaly can be obtained (Fig. 10). The amplitude difference in the Moho gravity anomaly in the study area is approximately 470 mGal, which indicates that the land area is low and that the sea area is high. The Moho gravity anomaly near the DFZ features a nearly SN-trending zone, which disrupts the continuity of the Moho gravity anomaly in the Zambezi Delta basin and its eastern area to a certain extent. In addition, the Moho gravity anomaly in the Beira High is lower than the surrounding anomalies.

The Moho gravity anomaly is subtracted from the Bouguer gravity anomaly to obtain the sedimentary layer gravity anomaly in the study area (Fig. 11). Because the density of the sedimentary layer in the Zambezi Delta basin is lower than that in the crust, theoretically, the variation in the sedimentary layer gravity anomaly has a good in-phase relationship with the undulation in the sedimentary basement interface (Mesozoic bottom interface). Based on these findings, we compared the seismic profile with the gravity anomaly profile extracted from the sedi-

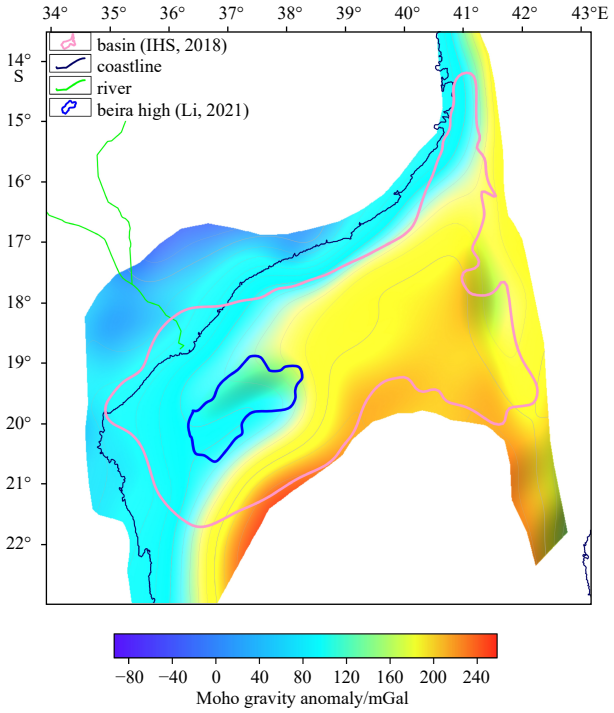

Fig. 10. Moho gravity anomaly in the study area.

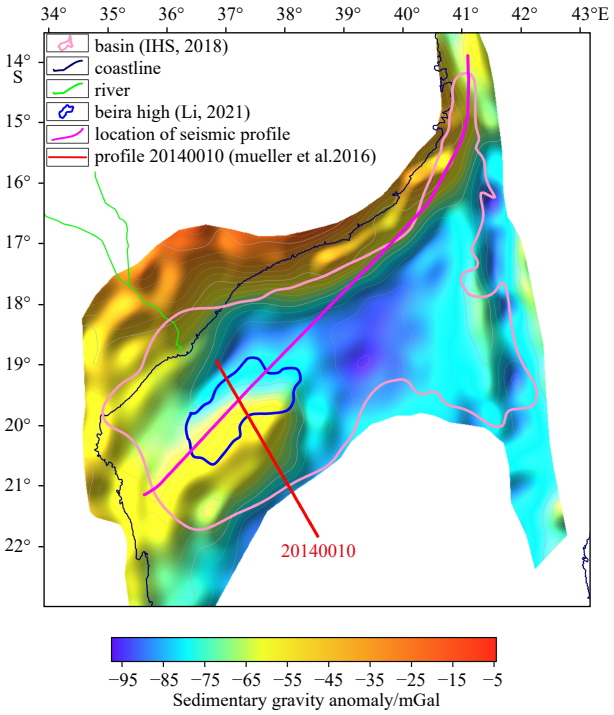

Fig. 11. Gravity anomaly of the sedimentary layer and the profile location.

mentary layer at the same location (Fig. 12; the location is shown by the purple solid line in Fig. 11). The sedimentary layer gravity anomaly and the sedimentary basement exhibit the same fluctuating characteristics in the same area, and the overall relationship occurs in phase, which proves that the extraction of sedimentary gravity anomalies in this study is appropriate. The gravity anomaly values of the sedimentary layer in the study area

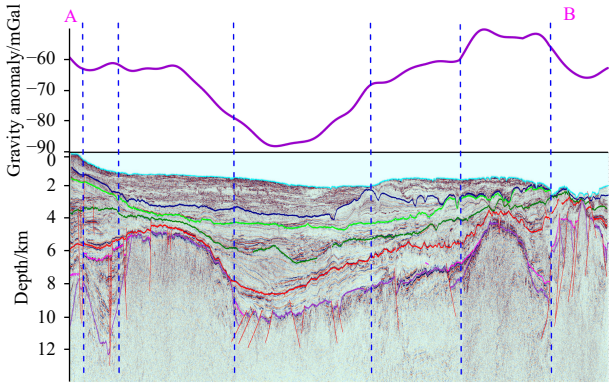

Fig. 12. Comparison of the gravity anomaly of the sedimentary layer and the Jurassic bottom interface.

range from –105 mGal to 0 mGal, which indicates that the overall gravity anomaly in the land area is greater than that in the sea area. The sedimentary gravity anomaly near the DFZ area shows a continuous nearly SN-trending band, the gravity anomaly in the Zambezi Delta basin is low, and the area of the Beira High has a relatively high gravity anomaly.

Owing to the special phenomenon in which the satellite altimetry gravity anomaly and Bouguer gravity anomaly exhibit relatively low gravity anomalies in the Beira High, we observe that the Moho interface gravity anomaly in the Beira High is relatively low, but the sedimentary layer gravity anomaly is relatively high. Based on these data, we extracted the Bouguer gravity anomaly, Moho gravity anomaly and sedimentary layer gravity anomalies (Fig. 13) at the location of the NW-trending Profile 20140010 on the Beira High (Fig. 11). The amplitude range of the Moho gravity anomaly in Profile 20140010 is 98 mGal to 252 mGal, and the amplitude range of the sedimentary layer gravity anomaly is –95 mGal to –54 mGal. The absolute value of the Moho gravity anomaly amplitude is much greater than that of the sedimentary gravity anomaly. Therefore, the Moho interface gravity anomaly at the Beira High has an "overcompensation" effect on the gravity anomaly in the sedimentary layer, resulting in relatively low values in the comprehensive response to gravity anomalies, such as satellite altimetry gravity anomalies and Bouguer gravity anomalies. As the density of the crust is lower than that of the mantle, theoretically, the Moho gravity anomaly and the fluctuation shape of the Moho interface should exhibit a good in-phase relationship; that is, the depression of the Moho interface will lead to a relatively low Moho gravity anomaly. In fact, interpretations from geological profiles have confirmed that the Moho interface is depressed at the location of the Beira High (Mueller et al., 2016). Therefore, it is inferred that the depression of the Moho interface in the Beira High results in relatively low Moho gravity anomalies and that "overcompensation" is generated for the sedimentary layer's gravity anomaly, resulting in a low satellite altimetry gravity anomaly and a low Bouguer gravity anomaly.

2.4.3 *Inversion method for the sedimentary basement interface*

The gravity anomaly in the sedimentary layer is a comprehensive response caused by fluctuations in the Cenozoic and Mesozoic strata. As the sedimentary basement interface, the Mesozoic bottom interface plays an important role in controlling the sedimentary evolution of the Zambezi Delta basin. To inverse the sedimentary basement interface, we need to forward model the Cenozoic stratigraphic gravity anomaly and eliminate it from the sedimentary gravity anomalies. When forward model-

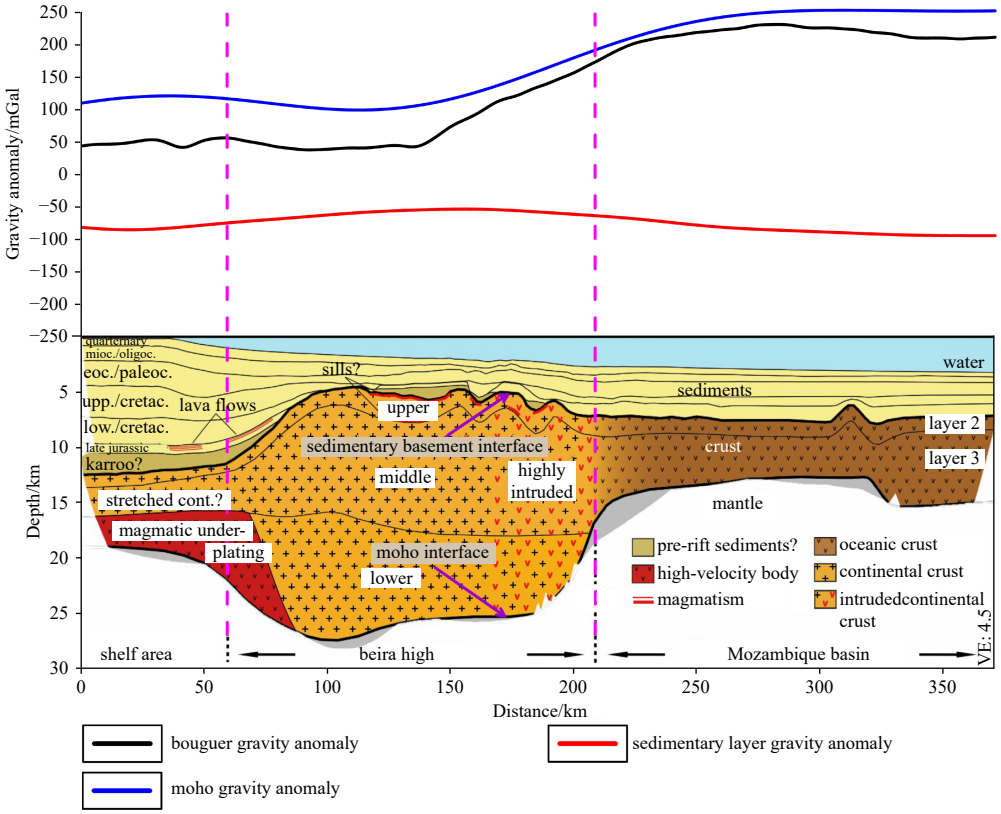

Fig. 13. Comparison of the geological profile (Mueller et al., 2016) and the gravity anomaly.

ing the Cenozoic stratigraphic gravity anomaly, we choose the zero plane as the upper interface and the fused bottom Cenozoic interface as the lower interface; additionally, we choose -0.30×10^3 kg/m^3 as the residual density of the Cenozoic strata relative to the Mesozoic strata. The Cenozoic stratigraphic gravity anomaly is calculated by using the fast forward method of the double-interface model of the gravity anomaly field (Wang and Pan, 1993), and then we obtain the Mesozoic gravity anomaly by removing it from the sedimentary gravity anomaly. When the fast inversion method of the double-interface model of the gravity anomaly field (Wang and Pan, 1993) was used to calculate the depth of the sedimentary basement interface based on the extracted Mesozoic gravity anomaly, the zero plane was selected as the upper interface, the fused Mesozoic bottom interface was selected as the lower interface (the initial interface of the sedimentary basement), -0.30×10^3 kg/m^3 was selected as the residual density of the Mesozoic strata relative to the crust, and the sedimentary basement interface was subsequently obtained (Fig. 14). On this basis, we calculated the thickness of the sedimentary strata in the study area (Fig. 15) by subtracting the terrain elevation from the depth of the sediment basement.

The sedimentary basement interface of the Zambezi Delta basin (Fig. 14) is mainly NE-trending and has a maximum depth reaching 14 km. In the eastern part of the basin, nearly SN-trending relief bands appear at the location of the DFZ. In the central basin, the basement depth of the Beira High is relatively shallow. The northern basement is deep and fluctuates greatly. In the eastern part, the overall burial depth is relatively small, and the fluctuation is small. The thickness of the sedimentary layer (Fig. 15) exhibits a NE trend and reaches a maximum of 14 km, with an average of approximately 6.3 km. There are two parallel shallow sedimentary bands that trend SN at the location of the DFZ. The thickness of the sedimentary layer on the northern side

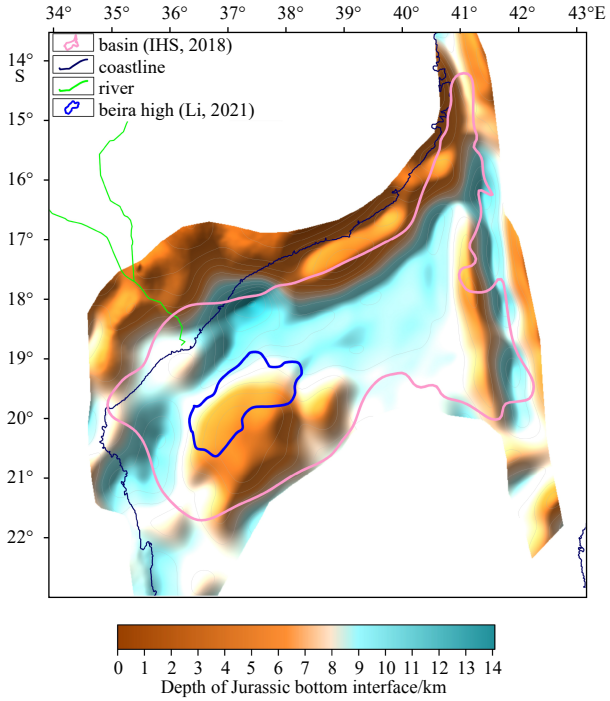

Fig. 14. Depth of the Jurassic bottom interface in the study area.

of the Beira High is relatively high and fluctuates greatly, while the overall thickness of the sedimentary layer on the eastern side fluctuates less. The Zambezi Delta basin has abundant sediment sources and a relatively stable sedimentary environment, which has formed a good reservoir and cap environment for the accumulation of oil and gas.

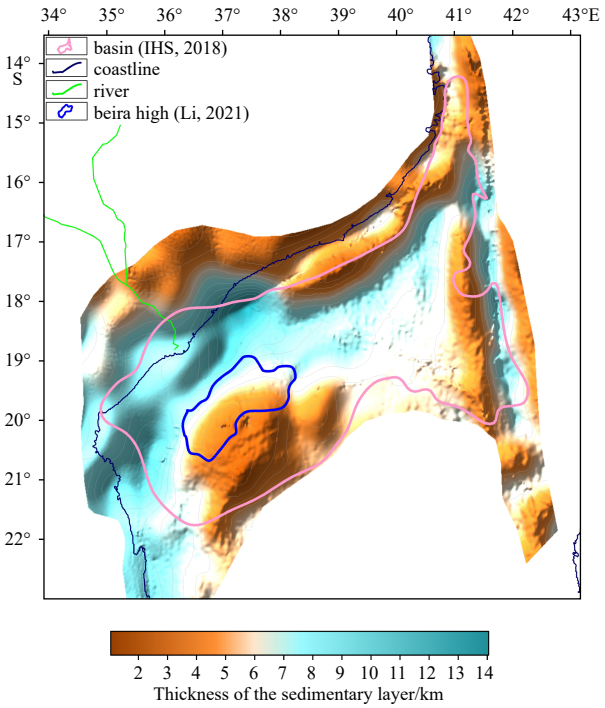

Fig. 15. Thickness of the sedimentary layer in the study area.

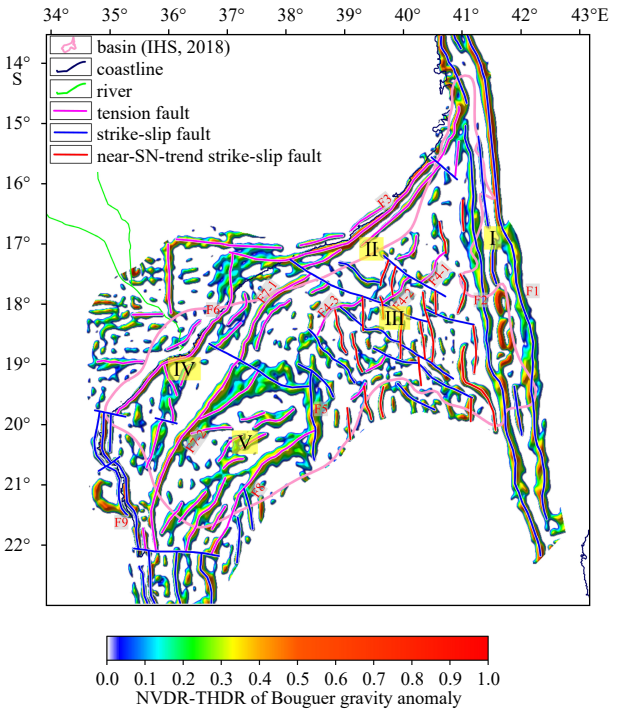

Fig. 16. The NVDR-THDR of the Bouguer gravity anomaly and the distribution of faults in the study area.

3 Structural characteristics of the Zambezi Delta basin

3.1 *Fault distribution characteristics*

The faults in the Zambezi Delta basin are well developed (Fig. 16) and are mainly distributed in NE-trending, NW-trending and nearly SN-trending. The properties and scale of the faults can be divided into tensile, strike-slip and nearly SN-trending strike-slip faults. In this study, we identify a total of 9 relatively large faults (Figs 16 and 17, F1–F9) in the study area; these faults trend nearly SN-trending and NE-trending and controlled the formation of 5 fault development zones in the whole basin. The faults in the study area exhibit a zonal development characteristic by east-west blocks, and the nearly SN-trending strike-slip faults F2, F5 and F9 have controlled the development of these blocks in the study area. The eastern part of the basin is bounded by fault F2 (a left branch of the DFZ), the western part is bounded by the strike-slip fault zone F9, and the central fault F5 divides the basin into eastern and western parts, in which the faults have developed differently. The detailed statistics about the locations and trends of the large-scale faults are presented in Table 2.

Macroscopically, the Zambezi Delta basin is divided into 5 fault development zones by 9 inferred large-scale extensional or strike-slip faults (Figs 16 and 17), and several smaller faults developed in each zone. The area between strike-slip fault F1 and fault F2 on the eastern side of the Zambezi Delta basin is fault development zone I (Davie fault zone), which has a narrow band-like shape with a nearly SN-trending. In fault development zone I, nearly SN-trending strike-slip faults developed, and the residual Bouguer gravity anomalies exhibit a chain–bead pattern. A possible reason is that the East Gondwana continent drifted southward along the DFZ in the Middle Jurassic, and a series of strike-slip faults parallel to faults F1 and F2 developed in the region, mainly by the influence of strike-slip action. During the drift, the East Gondwana continental block may have partially split and remained there, resulting in high residual Bouguer gravity anomaly values. The left branch of the DFZ (fault F2) is located on the eastern boundary of the Zambezi Delta basin and plays an important role in the stable sedimentary process of the Zambezi Delta basin. Fault development zone II is located south of tensile fault F3 and north of fault F4 and has a narrow strip-like shape and a large area. The area is mainly affected by NW trend tensile stress, and NE-trending tensile fractures are well developed. Fault F3 is located in the high-value zone of the residual

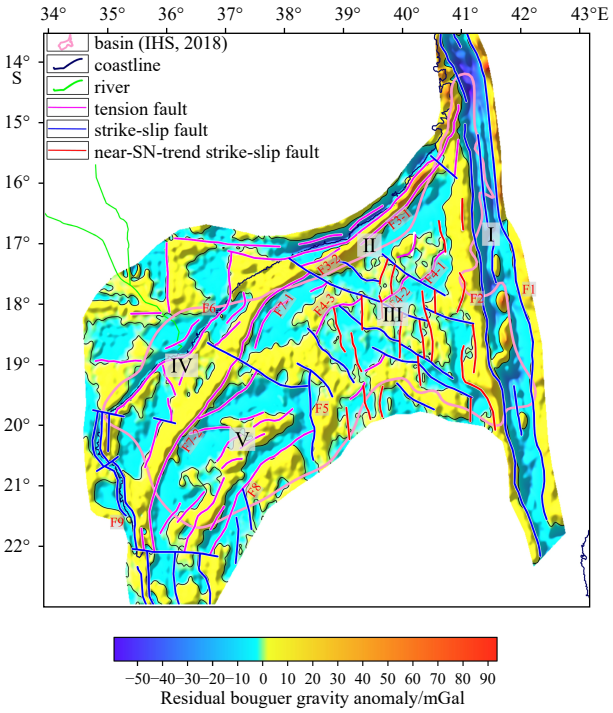

Fig. 17. Residual Bouguer gravity anomaly and fault distribution in the study area.

Table 2. Statistical table of the inferred results for the main faults

Number	Identifying characteristics	Trend	Position	Nature	Length/km
DFZ	NVDR-THDR continuous ridge value	nearly SN	east side of basin	strike-slip	–
F3	NVDR-THDR continuous ridge value	NE	north side of basin	tension	557
F4	NVDR-THDR continuous ridge value and local dislocation	NE	eastern part of the basin, which is centered	tension	259
F5	NVDR-THDR continuous ridge value	nearly SN	mid-basin	strike-slip	164
F6	NVDR-THDR continuous ridge value	nearly SN	northwestern basin	tension	392
F7	NVDR-THDR continuous ridge value	NE	north side of Beira High	tension	614
F8	NVDR-THDR continuous ridge value	NE	south side of Beira High	tension	305
F9	NVDR-THDR continuous ridge value	nearly SN	west side of basin	strike-slip	265

Bouguer gravity anomaly (Fig. 17), and a parallel tension fault system has developed nearby. It is inferred that this tension fault system was mainly affected by tensile stress during the Karoo intracontinental rift stage, followed by magma upwelling along the fault, which finally formed the Limpopo-Angoche dike (LADS) and caused a high-value zone in the residual Bouguer gravity anomaly. South of fault F3 and north of fault F4, high and low values alternate in the NE-trending on the residual Bouguer gravity anomaly and are truncated by NW-trending faults. The tectonic direction is mainly NE-trending, and the NE-trending tension faults in the area are sheared by NW-trending strike-slip faults. Small-scale nearly SN-trending distribution characteristics of NⅤDR-THDR data can be observed locally, suggesting that this area may be a transitional region in terms of fault development. This area mainly featured NW-trending tensile stress during the Karoo intracontinental rift and Gondwana continent breakup stages, which led to the formation of NE- and NW - trending faults. During the continental drift stage, some regions were subjected to nearly SN-trending stress caused by the southward drift of the Antarctic continent, resulting in the development of small faults with nearly SN trends. The northern end of the NW-trending shear fault in this area did not pass through the Limpopo-Angoche dike intrusion (LADS) because the NE-trending tension fault was generated by the NW-trending tensile stress during the Gondwana continent breakup stage. Due to the difference in rock properties and tensile stress, a NW-trending shear fault was also generated, and the Limpopo-Angoche dike prevented further northward development of the NW strike-slip fault. To the east of strike-slip fault F5, west of fault F2 and south of tension fault F4 is fault development zone Ⅲ, which is large in area and mainly features NW- and nearly SN-trending strike-slip faults. The scale of the NW-trending faults is relatively large, and these faults control the overall structural framework of the region. The scale of the nearly SN-trending faults is relatively small, and these faults, along with some shear NW-trending strike-slip faults, are scattered in fault development zone Ⅲ. The special fault development characteristics of fault development region Ⅲ may be controlled by the tectonic stress during different periods of Gondwanan continental breakup. In the early period, NW-trending tectonic stress controlled the development of NW-trending strike-slip faults. As the tectonic stress direction shifted to nearly SN-trending, the Antarctic continent drifted southward, generating nearly SN-trending tectonic stress in fault development region Ⅲ, forming a nearly SN-trending strike-slip faults and shearing the NW-trending faults. The area to the south of tension fault F6, north of fault F7 and east of strike-slip fault zone F9 is fault development zone Ⅳ, which is narrow and elongated, with a NE-trending strip-like distribution. The area is mainly affected by NW-trending tension stress, which formed the NE-trending tension fault system. The tension fault F7 is sheared by a NW-trending strike-slip fault, and fault development zone Ⅳ is divided into western and eastern sections. The western section is slightly wider and located in the low-value area of the residual Bouguer gravity anomaly, where NE-trending tension faults developed internally. The eastern section is slightly narrower, high and low residual Bouguer gravity anomaly values are alternately distributed in the region. Multiple parallel NE-trending tension faults have developed. The special characteristics of fault development in zone Ⅳ may be related to the Beira High. During the Gondwana continent breakup stage, the NW-trending tensile stress acted on fault development zone Ⅳ, and the existence of the Beira High caused uneven stress, leading to deformation in fault development zone Ⅳ. The western section was blocked by the Beira High, and the region was relatively stable and developed a single NE-trending tension fault. The eastern section experienced tensile stress during the Karoo rift stage and Gondwana continental rift stage, during which a parallel NE-trending tension fault system developed. The area between tension faults F7-2 and F8 is fault development zone Ⅴ, which is located on the Beira High and features a NE-trending block shape. It shows overall low values of the residual Bouguer gravity anomaly values in the fault development zone Ⅴ, with irregular banded high gravity anomalies are present in the middle of the area, and a series of small NE-trending faults exist nearby, which may be caused by local tectonic deformation on the Beira High under NW-trending tensile stress during the Gondwanan intercontinental rift stage.

The five fault development zones in the Zambezi Delta basin have their own characteristics, which are mainly manifested in the different development characteristics and complexities of the faults. Further study of the distribution characteristics of faults reveals that the fault has a zoning distribution feature of east-west blocks. To the east of the nearly SN-trending strike-slip fault F5, there are mainly NW- and nearly SN-trending strike-slip faults, while to the west of fault F5, NE-trending tension faults have developed. Based on the statistical analysis results of fault length and trend (Fig. 18), nearly NS-trending faults are the most common in the Zambezi Delta basin, followed by NE-trending faults, with less development of NWW-, NNW-, NNE- and NEE-

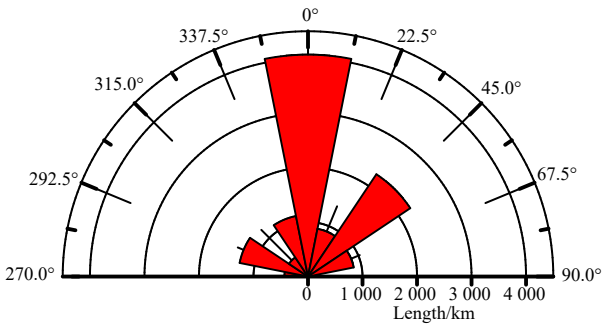

Fig. 18. Rose diagram of the fault length and trend.

trending faults, and few NW- and nearly EW-trending faults. Compared with previous research results, the location and trend of the NE-trending tension faults on the north side of the Beira High and the NW-trending shear faults in the middle of the basin identified in this study are basically consistent with previous studies, but the scale and continuity of the faults are different. In addition, this study reveals that the faults in the entire study area exhibit zoning development feature characterized by east-west blocks and briefly analyzes the possible reasons for the generation of the fault development characteristics in different regions.

3.2 *Distribution characteristics of uplift and depression patterns*

The Zambezi Delta basin was formed by tensile stress during the Karoo intracontinental rift stage and Gondwana continental breakup stage. The Beira High in the basin is an ancient uplifted landmass that remained on the basement during the southward drift of the Antarctic plate, and the sedimentary layers on it are relatively thin. In contrast, the basement of a depression undergoes downward deformation, usually leading to the development of thicker sedimentary layers. For the tectonic division of basins, several scholars have applied different classification criteria (Wang et al., 2009a; Zhou et al., 2010; Li et al., 2012; Feng et al., 2018). Based on the previous tectonic division criteria and combined with the specific geological characteristics of the Zambezi Delta basin, this study delineated the basin boundary mainly based on the contour line of a sedimentary thickness of 3 km on the landward side. On the seaward side, the trend of the sedimentary thickness is the main reference criterion, and the characteristics of gravity anomalies and fault development are secondary identifying characteristics and are used to make a comprehensive judgment. The division of the internal uplift and depression boundaries in the basin is based mainly on the change in sedimentary layer thickness, the characteristics of the fault trend and the relative fluctuations in the sedimentary basement are taken as references. Based on the criteria of the basin and the boundary between the uplift and depression, this study redefined the Zambezi Delta basin and its internal boundary between the uplift and depression (Fig. 19). The Zambezi Delta basin mainly trends NE and features uplift and depression characteristics in east-west blocks. The western block consists of the western depression and the Beira High and features the NE-trending distribution characteristics of a northern depression and a southern uplift. The western depression has a clumpy shape and a large area with a thick sedimentary layer. The thickest sedimentary layer in the whole basin is located at the northern end of the western depression, and the thickness of the sedimentary layer in the western depression is thick at both ends and thin in the middle. The southern uplift is the Beira High, which has an irregular clumpy shape and a large area. The sedimentary layer thickness is relatively small, and the shallowest part of the whole basin is located in the middle of the Beira High. The eastern block consists of the northern slope belt and the eastern depression, showing the overall characteristics of a NE-trending northern uplift and southern depression. The northern slope is a narrow strip with a small area, and its sedimentary layer thickness increases gradually from north to south. The eastern depression is an irregular quadrilateral in shape and has a large area. The basement is overlain by a sedimentary layer with a certain thickness and overall little undulation, and its thickness gradually decreases from north to south. Compared with previous research results (Fig. 20), the main direction of uplifts and depressions in this study is NE-trending. The distribution characteristics of the Beira High, located between the western depression

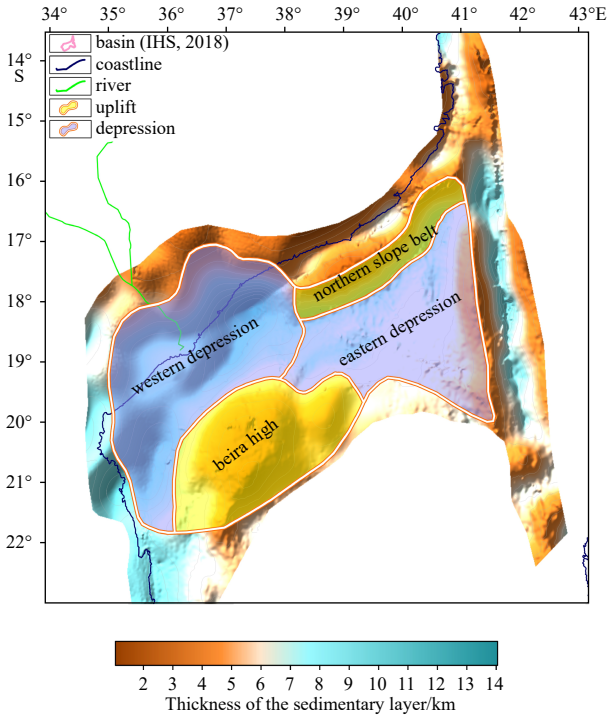

Fig. 19. Uplift and depression pattern in the study area.

(delta) and the eastern depression (submarine fan), are consistent, but the boundary positions of the uplift and depressions are different. In addition, the slope belt in the northern part of the basin was identified, expanding the area of the western depression and the Beira High and reducing the area of the eastern depression in this study.

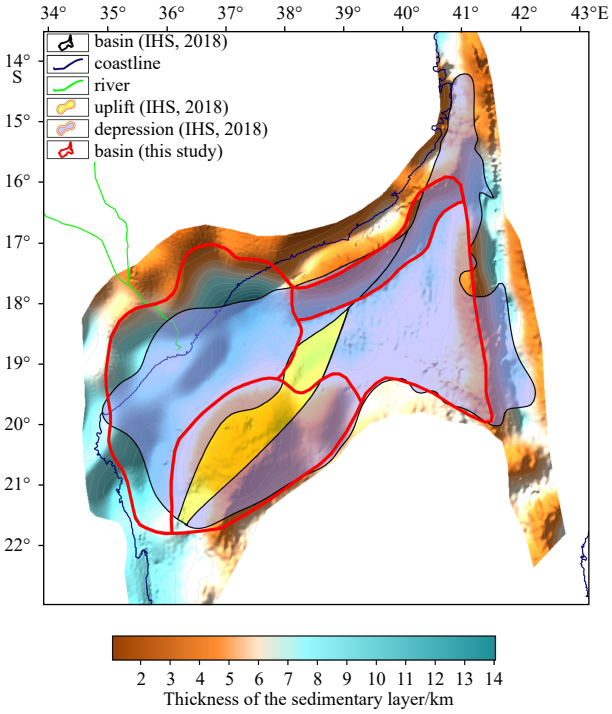

Fig. 20. Comparison of the distribution characteristics of uplifts and depressions with the results of previous studies in the study area.

4 Understanding of the tectonic framework and oil and gas distribution

The Zambezi Delta basin has good potential for oil and gas exploration, and the uplift of the sedimentary basement has formed anticlines and domes that have provided good traps for oil and gas. Faults can serve as channels or blocking structures for oil and gas migration. Faults, uplifts and depressions are closely related to the distributions of oil and gas, so comprehensive research on the tectonic patterns of faults, uplifts and depressions is needed.

The tectonic framework of the Zambezi Delta basin (Fig. 21) reveal that the tectonic framework of the basin is mainly oriented NE, and the faults controlled the uplift and depressions, forming east-west block tectonic characteristics. The nearly SN-trending left branch of the DFZ (fault F2) and strike-slip fault F9 are located near the eastern and western boundaries of the basin, respectively, providing a stable sedimentary environment for the basin. The development of the nearly SN-trending strike-slip fault F5 in the basin provided a relatively independent tectonic evolutionary environment for the eastern and western tectonic units, which inevitably led to differences in the structural characteristics of the eastern and western blocks and further affected the differences in oil and gas distribution patterns.

Based on the understanding of hydrocarbon accumulation patterns in passive continental margin basins along the East African coast, it is believed that the combination of traps formed by deltas with source-connected faults and deep-water turbidite fan sand bodies in the sea may have great potential for oil and gas exploration (Cui et al., 2020). Combined with the collected oil and gas well data (IHS, 2018; the oil and gas well are shown in Fig. 21), further analysis reveals that oil and gas well concentration areas A and B have similar structural characteristics: both are located in depressions with thick sedimentary layers and have a certain scale of protrusions and nearby faults. In the western block of the Zambezi Delta basin, the tension fault F7 controlled the development of the western depression and the Beira High, forming a tectonic pattern with a northern depression and southern uplift. Fault development zone IV is located in the western depression, the NE-trending tension faults F6 and F7 controlled the western depression and the fault system is mainly oriented NE, and the sedimentary strata are thick. It is speculated that the tectonic units that formed during the Karoo Rift period were subjected to NW-trending tensile stress, resulting in a series of extensional faults controlling the formation of the NE-trending Zambezi Graben. During the intracontinental rift and continental drift stages in Gondwana, a relatively stable sedimentary environment was provided by the obstruction of the Beira High on the southern side, where a large amount of sediment carried by the Zambezi River was deposited, forming a western depression (Zambezi Delta) with thick sedimentary layers. The relatively stable sedimentary environment and thick sedimentary layers provided the necessary conditions for the formation of good reservoirs and cap layers in the western depression. Vertically, the tension fault in the western depression passes through the sedimentary basement, which may have formed a through-source fault (Fig. 9). Laterally, the tension fault traverses concentrated areas A and B of oil and gas wells. Moreover, the connection between the tension fault F6 with the strike-slip fault F9 passing through zone A may have acted as a channel for oil and gas migration or a blocking structure. A certain scale of protrusions, such as anticlines and domes, may have developed within the western depression, possibly leading to the formation of trap structures; therefore, oil and gas may have accumulated in reservoirs within the western depression. In the eastern block of the Zambezi Delta basin, the tension fault F3 and its nearby fault structural system controlled the northern slope and the eastern depression, forming a tectonic pattern involving a northern uplift and a southern depression. Fault development zone III is located in the eastern depression and features mainly NW- and nearly SN-trending strike-slip faults within sedimentary cover with a certain thickness with little undulation, this zone has the potential to form reservoirs and cap layers. However, there are almost no bulges in the eastern depression, making it difficult to form oil and gas traps associated with structural domes.

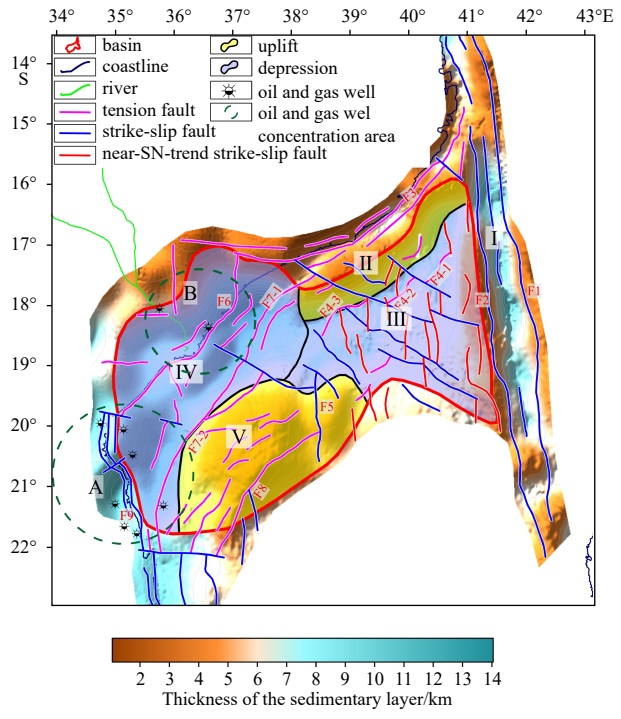

Fig. 21. Oil and gas well distribution characteristics and tectonic framework map of the study area.

5 Conclusions

This study focuses on the structural characteristics of faults, uplifts and depressions in the Zambezi Delta basin. Aiming to solve the problem of low gravity anomaly values associated with the Beira High caused by the special geological evolutionary background in the Zambezi Delta basin, we propose a set of technical schemes to inverse the sedimentary basement based on the constraints of seismic data. For the first time, the sedimentary layer gravity anomaly extraction technique under the seismic data constraints, the fault identification technique and the sedimentary basement interface inversion technique were applied to the Zambezi Delta basin. The distribution characteristics of faults, uplifts and depressions are accurately evaluated, and good results are achieved through the joint interpretation of gravity and seismic data.

Through the joint processing and interpretation of gravity anomalies and seismic data from the Zambezi Delta basin, it has been proven that the low gravity anomaly at the Beira High in the study area represents an “overcompensation” phenomenon caused by the gravity anomaly generated by depression of the Moho interface to the gravity anomaly of the sedimentary layer.

The Zambezi Delta basin boundary is reidentified, and the uplift and depression distribution characteristics are characterized as east-west blocks. It is inferred that the faults in the basin are mainly in NE-trending and can be divided into east-west blocks. A NE-trending tension fault structural system formed in the western depression, with faults passing vertically through the sedimentary basement and laterally through areas concentrated oil and gas wells. Thus, these faults may have acted as channels for oil and gas migration or as blocking structures, resulting in great oil and gas exploration potential. This depression is the preferred area for oil and gas exploration in the Zambezi Delta basin.

References

An Yulin, Zhang Minghua, Huang Jinming, et al. 2010. The computation scheme and computation process for gravity correction values within the pure spherical coordinate system. Geophysical and Geochemical Exploration (in Chinese), 34(6): 697–705

Castelino J A, Reichert C, Klingelhoefer F, et al. 2015. Mesozoic and Early Cenozoic sediment influx and morphology of the Mozambique Basin. Marine and Petroleum Geology, 66: 890–905, doi: 10.1016/j.marpetgeo.2015.07.028

Cox K G. 1992. Karoo igneous activity, and the early stages of the break-up of Gondwanaland. Geological Society, London, Special Publications, 68(1): 137–148

Cui Ge, Jin Aimin, Wu Changwu, et al. 2020. Tectonic evolution of East Africa coast and comparison of hydrocarbon accumulation conditions in the north and south petroliferous basins. Marine Geology & Quaternary Geology (in Chinese), 40(1): 104–113, doi: 10.16562/j.cnki.0256-1492.2018080103

Cui Zhihua, Lou Zhanghua, Zhu Zhenhong, et al. 2016. Petroleum geological characteristics and exploration prospect of Mozambique basin. Marine Geology Frontiers (in Chinese), 32(6): 1–8,22, doi: 10.16028/j.1009-2722.2016.06001

Feng Xuliang, Zhang Gongcheng, Wang Wanyin, et al. 2018. An integrated study on distribution of Cenozoic basins in the South China Sea based on gravity, magnetic and seismic data. Chinese Journal of Geophysics (in Chinese), 61(10): 4242–4254, doi: 10.6038/cjg2018L0567

He Tao, Wang Wanyin, Bai Zhizhao, et al. 2023. Integrated gravity and magnetic study on patterns of petroleum basin occurrence in the China seas and adjacent areas. Acta Oceanologica Sinica, 42(3): 201–214, doi: 10.1007/s13131-022-2139-5

IHS. 2018. International energy oil & gas industry solutions. http://www.ihs.com/industry/oil-gas/internation.aspx

Ji Xiaolin, Wang Wanyin, Qiu Zhiyun. 2015. The research to the minimum curvature technique for potential field data separation. Chinese Journal of Geophysics (in Chinese), 58(3): 1042–1058, doi: 10.6038/cjg20150329

Jin Chong, Chen Anqing, Lou Zhanghua, et al. 2012. Tectonic evolution and hydrocarbon accumulation principle in East Africa. Journal of Jilin University (Earth Science Edition) (in Chinese), 42(S2): 121–130, doi: 10.13278/j.cnki.jjuese.2012.s2.012

Jourdan F, Bertrand H, Féraud G, et al. 2009. Lithospheric mantle evolution monitored by overlapping large igneous provinces: case study in southern Africa. Lithos, 107(3-4): 257–268, doi: 10.1016/j.lithos.2018.10.011

Jourdan F, Féraud G, Bertrand H, et al. 2007. Distinct brief major events in the Karoo large igneous province clarified by new $^{40}Ar/^{39}Ar$ ages on the Lesotho basalts. Lithos, 98(1-4): 195–209, doi: 10.1016/j.lithos.2007.03.002

König M, Jokat W. 2010. Advanced insights into magmatism and volcanism of the Mozambique Ridge and Mozambique Basin in the view of new potential field data. Geophysical Journal International, 180(1): 158–180, doi: 10.1111/j.1365-246X.2009.04433.x

Lei Shoumin. 1984. Calculation of generalized topographic and isostatic gravity corrections. Marine Geology & Quaternary Geology (in Chinese), 4(1): 101–111, doi: 10.16562/j.cnki.0256-1492.1984.01.013

Leinweber V T, Klingelhoefer F, Neben S, et al. 2013. The crustal structure of the Central Mozambique continental margin - Wide-angle seismic, gravity and magnetic study in the Mozambique Channel, Eastern Africa. Tectonophysics, 599: 170–196, doi: 10.1016/j.tecto.2013.04.015

Li He. 2021. Crustal architecture and Tectonic-sedimentary evolution of the transform continental margin: insights from the Southern Mozambique Margin, East Africa (in Chinese)[dissertation]. Hangzhou: Zhejiang University, doi: 10.27461/d.cnki.gzjdx.2021.002613

Li Jinbo, Wu Guiqian, Xu Chuang, et al. 2023. Influence of gravity stripping in the South China Sea area on Moho inversion. Progress in Geophysics (in Chinese), 38(1): 0031–0046, doi: 10.6038/pg2023gg0083

Li Yuejun, Yang Haijun, Zhang Guangya, et al. 2012. Redivision of the tectonic units of tabei rise in tarim basin, NW china. Acta Petrologica Sinica (in Chinese), 28(8): 2466–2478

Luo Xin'gang, Wang Wanyin, Chen Ying, et al. 2023. Study on the distribution characteristics of faults and their control over petroliferous basins in the China seas and its adjacent areas. Acta Oceanologica Sinica, 42(3): 227–242, doi: 10.1007/s13131-022-2138-6

Mahanjane E S. 2012. A geotectonic history of the northern Mozambique Basin including the Beira High - A contribution for the understanding of its development. Marine and Petroleum Geology, 36(1): 1–12, doi: 10.1016/j.marpetgeo.2012.05.007

Mahanjane E S. 2014. The Davie Fracture Zone and adjacent basins in the offshore Mozambique Margin – A new insights for the hydrocarbon potential. Marine and Petroleum Geology, 57: 561–571, doi: 10.1016/j.marpetgeo.2014.06.015

Mahanjane E S, Franke D, Lutz R, et al. 2014. Maturity and petroleum systems modelling in the offshore Zambezi Delta depression and Angoche Basin, northern Mozambique. Journal of Petroleum Geology, 37(4): 329–348, doi: 10.1111/jpg.12589

Mueller C O, Jokat W. 2017. Geophysical evidence for the crustal variation and distribution of magmatism along the central coast of Mozambique. Tectonophysics, 712–713: 684–703, doi: 10.1016/j.tecto.2017.06.007

Mueller C O, Jokat W. 2019. The initial Gondwana break-up: a synthesis based on new potential field data of the Africa-Antarctica Corridor. Tectonophysics, 750: 301–328, doi: 10.1016/j.tecto.2018.11.008

Mueller C O, Jokat W, Schreckenberger B. 2016. The crustal structure of Beira High, central Mozambique-Combined investigation of wide-angle seismic and potential field data. Tectonophysics, 683: 233–254, doi: 10.1016/j.tecto.2016.06.028

Ponte J P, Robin C, Guillocheau F, et al. 2019. The Zambezi delta (Mozambique channel, East Africa): high resolution dating combining bio- orbital and seismic stratigraphies to determine climate (palaeoprecipitation) and tectonic controls on a passive margin. Marine and Petroleum Geology, 105: 293–312, doi: 10.1016/j.marpetgeo.2018.07.017

Rajesh R, Kumar K S, Tiwari R K. 2020. Regional and residual gravity anomaly separation using singular spectrum based frequency filtering methods: a case study of shallow subsurface modeling from Nagpur, India. Pure and Applied Geophysics, 177(2): 977–990, doi: 10.1007/s00024-019-02289-y

Salman G, Abdula I. 1995. Development of the Mozambique and Ruvuma sedimentary basins, offshore Mozambique. Sedimentary Geology, 96(1–2): 7–41, doi: 10.1016/0037-0738(95)00125-R

Sandwell D T, Müller R D, Smith W H F, et al. 2014. New global marine gravity model from CryoSat-2 and Jason-1 reveals buried tectonic structure. Science, 346(6205): 65–67, doi: 10.1126/science.1258213

Senkans A, Leroy S, d'Acremont E, et al. 2019. Polyphase rifting and break-up of the central Mozambique margin. Marine and Petroleum Geology, 100: 412–433, doi: 10.1016/j.marpetgeo.2018.10.035

Shi Buqing, Ding Liangbo, Ma Hongxia, et al. 2023. Characteristics of hydrocarbon accumulation in deep-water depositional system in offshore East Africa. Lithologic Reservoirs (in Chinese), 35(6): 10–17, doi: 10.12108/yxyqc.20230602

Solomon S, Bureau-Cauchois G, Ahmed N, et al. 2014. CO_2 storage capacity assessment of deep saline aquifers in the Mozambique Basin. Energy Procedia, 63: 5266–5283, doi: 10.1016/j.egypro.2014.11.558

Wang Buqing, Huang Zhibin, Ma Peiling, et al. 2009a. Establishment of division standard, evidence and principle of structural units in Tarim Basin. Geotectonica et Metallogenia (in Chinese), 33(1): 86–93, doi: 10.16539/j.ddgzyckx.2009.01.024

Wang Wanyin, Pan Zuoshu. 1993. Fast solution of forward and inverse problems for gravity field in a dual interface model. Geophysical Prospecting for Petroleum (in Chinese), 32(2): 81–87,123

Wang Wanyin, Pan Yu, Qiu Zhiyun. 2009b. A new edge recognition technology based on the normalized vertical derivative of the total horizontal derivative for potential field data. Applied Geophysics, 6(3): 226–233, doi: 10.1007/s11770-009-0026-x

Watts A B. 2001. Gravity anomalies, flexure and crustal structure at the Mozambique rifted margin. Marine and Petroleum Geology, 18(4): 445–455, doi: 10.1016/s0264-8172(00)00079-9

Wen Zhixin, Wang Zhaoming, Song Chengpeng, et al. 2015. Structural architecture difference and petroleum exploration of passive continental margin basins in East Africa. Petroleum Exploration and Development (in Chinese), 42(5): 671–680, doi: 10.11698/PED.2015.05.16

Xu Zhigang, Han Wenming, Sun Yumei. 2014. Tectonic evolution and petroleum exploration prospect of East Africa. Geology in China (in Chinese), 41(3): 961–969

Xu Chuang, Luo Zhicai, Sun Rong, et al. 2018. Multilayer densities using a wavelet-based gravity method and their tectonic implications beneath the Tibetan Plateau. Geophysical Journal International, 213(3): 2085–2095, doi: 10.1093/gji/ggy110

Yu Xuan, Hou Guiting, Dai Shuanghe, et al. 2015. Tectonic evolution and hydrocarbon pooling patterns analysis in East Africa continental margin. Geological Science and Technology Information (in Chinese), 34(6): 147–154,158

Zhang Gongcheng, Feng Yangwei, Qu Hongjun. 2022. Characteristics of petroleum geology of global five deep-water basin belts. China Petroleum Exploration (in Chinese), 27(2): 11–26, doi: 10.3969/j.jssn.1672-7703.2022.02.002

Zhang Yimi, Wang Wanyin, Li Linzhi, et al. 2023. Influence of the Moho surface distribution on the oil and gas basins in China seas and adjacent areas. Acta Oceanologica Sinica, 42(3): 167–188, doi: 10.1007/s13131-022-2136-8

Zhou Xinhuai, Yu Yixin, Tang Liangjie, et al. 2010. Cenozoic offshore basin architecture and division of structural elements in Bohai sea. China Offshore Oil and Gas (in Chinese), 22(5): 285–289